ORIGINAL ARTICLE

Annals of Nuclear Medicine Vol. 15, No. 6, 487–494, 2001

The CdTe detector module and its imaging performance

Issei MORI, Takuzo TAKAYAMA and Nobutoku MOTOMURA

Medical Systems R&D Center, Toshiba Corporation Medical Systems Company

In recent years investigations into the application of semiconductor detector technology in gamma cameras have become active world-wide. The reason for this burst of activity is the expectation that the semiconductor-based gamma camera would outperform the conventional Anger-type gamma camera with a large scintillator and photomultipliers. Nevertheless, to date, it cannot be said that this expectation has been met. ***Methods:*** While most of the studies have used CZT (Cadmium Zinc Telluride) as the semiconductor material, we designed and fabricated an experimental detector module of CdTe (Cadmium Telluride). The module consists of 512 elements and its pixel pitch is 1.6 mm. We have evaluated its energy resolution, planar image performance, single photon emission computed tomography (SPECT) image performance and time resolution for coincidence detection. ***Results:*** The average energy resolution was 5.5% FWHM at 140 keV. The intrinsic spatial resolution was 1.6 mm. The quality of the phantom images, both planar and SPECT, was visually superior to that of the Anger-type gamma camera. The quantitative assessment of SPECT images showed accuracy far better than that of the Anger-type camera. The coincidence time resolution was 8.6 ns. All measurements were done at room temperature, and the polarization effect that had been the biggest concern for CdTe was not significant. ***Conclusion:*** The results indicated that the semiconductor-based gamma camera is superior in performance to the Anger-type and has the possibility of being used as a positron emission computed tomography (PET) scanner.

Key words: semiconductor, detector, single photon emission computed tomography, energy resolution, cadmium telluride

INTRODUCTION

THE USE OF SEMICONDUCTOR DETECTORS with Silicon (Si) or Germanium (Ge) has been an established technology for radiation measurement. Unfortunately Si has an atomic number too low for sufficient stopping power, and Ge requires a special operating environment because of its need for cryogenic cooling. Therefore, for many years new materials with higher atomic numbers and operational at room temperature have been investigated by various researchers.[1] Among the candidates for detector material, the most promising ones have been CZT (Cadmium Zinc Telluride) and CdTe (Cadmium Telluride). In recent years progress in material technology has reduced the cost of these materials to more reasonable levels, so that investigations into the use of semiconductor detectors in gamma cameras have become very active,[2–4] with the expectation that gamma cameras with semiconductor detectors would, in several areas, outperform conventional gamma cameras based on the Anger principle.

Possible advantages of the semiconductor-based gamma camera include a thin, lightweight camera head, higher energy resolution and resulting superior image quality, higher spatial resolution owing to the pixellated structure, and a higher count rate owing to modular electronics. Among these, a thin, lightweight CZT camera head has been produced by Butler and Lingren, et al.[2]

The most significant possibility, however, is improved imaging performance resulting from the inherent high-energy resolution of the semiconductor detector. In areas such as astronomy, semiconductor detectors are already showing superb energy resolution. In gamma-camera applications, despite much work being done, only one

Received May 15, 2001, revision accepted August 24, 2001.

For reprint contact: Issei Mori, CT & Nuclear Medicine Systems Development Department, Medical Systems R&D Center, Toshiba Corporation Medical Systems Company, 1385, Shimoishigami, Otawara-shi, Tochigi 324–8550, JAPAN.

E-mail: itsusei.mori@toshiba.co.jp

study to date has shown satisfactory energy resolution.[3] The detector in this case was only 4 × 4 pixels in size, and, to our knowledge, other studies on semiconductor detectors with larger fields of view (FOVs) have so far achieved energy resolution only slightly better than that of the Anger-type gamma camera.

In this study we designed and constructed a new semiconductor detector module with the objective of improving imaging performance. The material is CdTe and has a blocking-contact electrode,[5,6] whereas CZT with ohmic-contact electrodes have been more preferred for nuclear medicine application thus far.

The module consists of 512 (16 × 32) CdTe elements. The most significant difference in the detector module design from those reported in the past for nuclear medicine is the electrode direction. We adopted a vertical electrode structure for better and faster charge collection, as opposed to the horizontal electrode structure with the electrode on the surface of the gamma-ray incidence.

We previously reported the basic performance tests on this new semiconductor module.[7,8] In this paper, the basic performance was re-evaluated with different methods and the use of a CdTe detector in a SPECT system was examined also. In addition, for use in PET, the coincidence time resolution for positron annihilation gammarays was measured.

MATERIALS AND METHODS

Design of detector element and detector module

Sixteen detector elements were slotted on a slab of single crystal CdTe. On one side of the slab, a layer of Platinum (Pt) was deposited as the common-bias electrode. On the other side, a layer of Indium (In) was deposited as the signal-readout electrode. Pt and In were chosen for their ability to form blocking contact by which to suppress dark (leakage) current. The details of the crystal growth and the mechanical/thermal/chemical processes have been described previously.[5,6] After forming the single crystal slab, the inside was slotted mechanically into 16 separate elements. The slab was 1.3 mm thick, 8 mm height and 25.6 mm long. The 512 element module consisted of 32 such slabs placed side-by-side (Fig. 1). Between the slabs, a common-bias plate, an insulating layer and 16 independent signal contacts were sandwiched. After assembling the 32 slabs and their contacts, the two ends of the module were reinforced with plastic plates and fastened together lightly with screws. The applied common-bias voltage was −1000 V. Among the 512 elements, some had excessive levels of dark current. Of those, we decided not to use 13 elements that had currents higher than 15 nA, even though at least some of them may have been functional. For imaging, data from these "defective" elements were compensated for by bilinear interpolation of data from neighboring elements.

Front end electronics and data acquisition system

We developed an application specific integrated circuit (ASIC) to handle the detector output. The ASIC is manufactured by IDE-AS (Norway), and one unit contains front end circuits and read out circuits for 128 detector elements. The front end circuit consists of the following:

(a) A low noise charge amplifier;
(b) A fast signal shaper with a short time constant that sends an event triggered pulse;
(c) A slow signal shaper with a relatively long time constant (variable, 1 microsecond optimum for our detector) that outputs the total charge per event;
(d) A read out circuit that selects the slow shaper and outputs its signal level.

Four ASICs were used to process the output from one detector module. Output signals from the ASICs were converted from analog to digital and transferred to a PC-based data acquisition system.

Energy resolution measurement

The energy spectrum was measured with a Tc-99m point source (140 keV). The 3.7 MBq source was placed 100 mm from the detector module. No collimator was used. To measure the correction constant for each element that

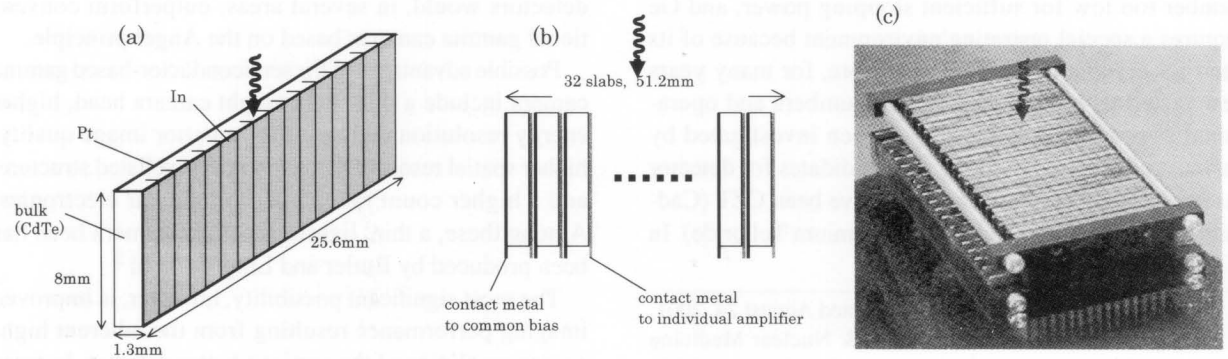

Fig. 1 Detector structure. (a) One slab consists of sixteen detector elements. (b) One module consists of 32 slabs with common-bias plates, signal readout contact pins and insulating layers. (c) External appearance of the CdTe detector module with 512 elements.

was required to convert the ASIC output to input radiation energy, a spectrum with a Co-57 source (122 keV) was taken separately.

Intrinsic spatial resolution measurement

We manufactured a bar phantom with 1.6 mm wide lead bars separated by 1.6 mm gaps. This bar phantom was placed on top of the detector module. The spatial frequency of this phantom coincided with the Nyquist frequency of the 1.6 mm pitch detector, so that the bar axis was tilted 45 degrees from that of the module to avoid aliasing. This phantom was irradiated with a Tc-99m 185 MBq point source located at a distance of 500 mm. Again, no collimator was employed.

LSF measurement with collimator

As a line source, a plastic tube with an inside diameter of 1 mm and filled with Tc-99m (185 MBq) was used. A low energy, high resolution collimator (Toshiba LEHR) was used with a hole diameter of 1.78 mm, septa thickness of 0.17 mm and hole depth of 40 mm. Line spread function (LSF) was measured at various distances, from 5 to 150 mm between the collimator surface and the line source.

Sensitivity measurement

The sensitivity was measured with a Tc-99m point source (140 keV). The 3.7 MBq source was placed 100 mm from the detector module. The collimator was an LEHR. The energy window was about 10% of the full width (14 keV) or about double that of the full width at half maximum (FWHM). For comparison, the same data were acquired with an Anger-type gamma camera (Toshiba GCA-9300A) with the same LEHR collimator and the same acquisition time, but with the energy window at 20% of the full width, which is double that of the FWHM.

Planar image acquisition

For planar imaging, we used an "IMP brain phantom" (SPECT brain phantom IB-30, Kyoto Kagaku Co. Ltd., Kyoto, Japan). Tc-99m injected into the IMP brain phantom was 155.8 MBq/550 m*l* for the gray-matter region and 27.57 MBq/350 m*l* for the white matter region. The LEHR collimator was used again. The phantom surface was 50 mm from the collimator surface. FOV of the CdTe detector module is only 1″ by 2″; so that data acquisition was performed section by section to cover the entire phantom. Acquisition time was 10 minutes per section. A total of 28 sections were acquired and tiled together after time decay correction. The energy window was about 10% of the full width (14 keV) or about double that of the FWHM. Before the imaging, sensitivity distribution data were obtained with a flood source. The sectional images were calibrated by means of the sensitivity data before tiling. For comparison, the same image was taken by an Anger-type gamma camera with the same LEHR collimator and the same acquisition time, but with the energy

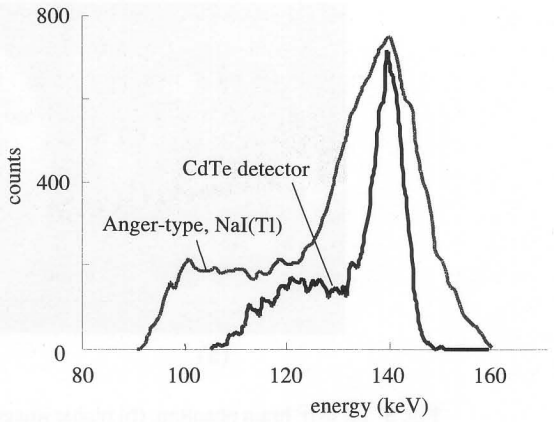

Fig. 2 The energy spectrum of the CdTe detector element with FWHM of 5.16% at 140 keV. For comparison, the energy spectrum of the NaI detector with FWHM of 10% is superposed. Vertical axis shows the count normalized by the peak level and thus irrelevant to the sensitivity.

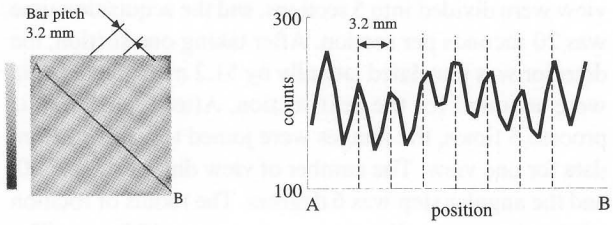

Fig. 3 The intrinsic spatial resolution of 1.6 mm is demonstrated. The pitch of the detector array is 1.6 mm both horizontally and vertically. The width of the lead bar is 1.6 mm and the pitch is 3.2 mm. The lead bars are positioned diagonally on the surface of the detector module. Count profile curve is also shown.

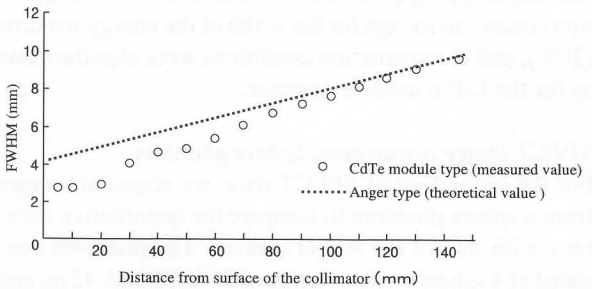

Fig. 4 Spatial resolution or FWHM of line source image as a function of distance. The collimator is LEHR. The ability of the CdTe detector to better resolve smaller structures is clear when the distance between the line source and the detector is smal.

window at 20% of the full width, which is double that of the FWHM.

SPECT image acquisition, IMP brain phantom

For the first set of SPECT images, the same IMP brain phantom as in the planar imaging was used. The energy

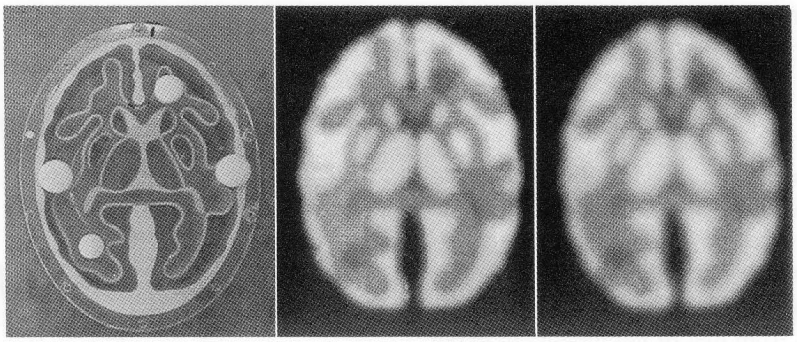

(a) (b) (c)

Fig. 5 (a) IMP brain phantom, (b) planar image by CdTe detector module and (c) image by Anger-type. The distance from phantom surface to collimator surface was 50 mm. Collimator was the LEHR. The energy window is 10% for CdTe and 20% for Anger-type. The image of CdTe detector (b) is superior in contrast and sharpness than that of Anger-type (c).

window was also the same. The image matrix was 128 by 128 for FOV of 250 mm (1.95 mm/pixel). Data for one view were divided into 5 sections, and the acquisition time was 20 seconds per section. After taking one section, the detector was translated laterally by 51.2 mm, and the data were acquired for the next section. After repeating this process 5 times, the images were joined together to form data for one view. The number of view directions was 60, and the angular step was 6 degrees. The radius of rotation of the detector collimator surface was 132 mm. The preprocessing filter was an order 8 Butterworth and the cutoff frequency was 0.14 cycle/pixel. The reconstruction filter for the filtered back projection method was a ramp filter. Scatter correction was not applied, but Sorenson's attenuation correction was. An LEHR collimator was used. For comparison, the same image was acquired with the Anger-type gamma camera under the same acquisition conditions except for the width of the energy window (20%), and reconstruction conditions were also the same as for the CdTe module detector.

SPECT image acquisition, sphere phantom

For the second set of SPECT data, we acquired images from a sphere phantom to compare the quantitative accuracy with that of the Anger camera. The phantom consisted of 4 spheres with volumes of 71 m*l*, 56 m*l*, 42 m*l* and 15 m*l* inside a cylinder with a diameter of 200 mm and a length of 200 mm. All spheres were located on the same radius from the center of the outer cylindrical phantom. The 15 m*l* sphere contained Tc-99m of 8.36 MBq, acting as a hot region, and the other spheres contained only water and no radioisotope, acting as cold regions. In the cylinder, Tc-99m of 925 MBq/6200 m*l* was injected as a background warm region. For data acquisition, the radius of rotation of the detector collimator surface was 132 mm. Sorenson's method was used to correct for attenuation, and the attenuation coefficient was assumed to be 0.15 cm^{-1}. The collimator was the LEHR. Other SPECT parameters for acquisition and image reconstruction were the same as those for the IMP brain phantom. The same image was taken with an Anger-type gamma camera with the same imaging protocol except for the 20% energy window. No scatter correction was applied to data from the CdTe detector because the experimental processing system on PC was not fully compatible with the TEW method.

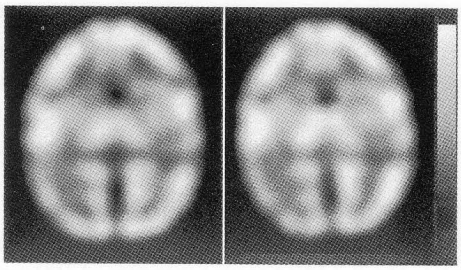

(a) (b)

Fig. 6 (a) SPECT image by CdTe detector module and (b) image by Anger-type. The detector rotation radius was 132 mm. Collimator was the LEHR. The energy window is 10% for CdTe and 20% for Anger-type. The image of CdTe detector (a) is slightly superior in contrast than that of Anger-type (b).

Coincidence time resolution measurement

For coincidence measurements, we used two matchstick-shaped CdTe detectors instead of the aforementioned detector module and used a dual-charge amplifier instead of the ASIC. The detector dimension was $1.35 \times 1.47 \times 8$ mm^3. The dual-charge amplifier was a 5529 from Clear Pulse, Inc. (Japan). To measure coincidence, the two CdTe detectors were placed in parallel at a distance of 10 mm, and a point source of Na-22 was placed between them. The outputs from the charge amplifiers were observed with a LeCroy digital oscilloscope LC584A, and a leading-edge triggering method was used. Specifically,

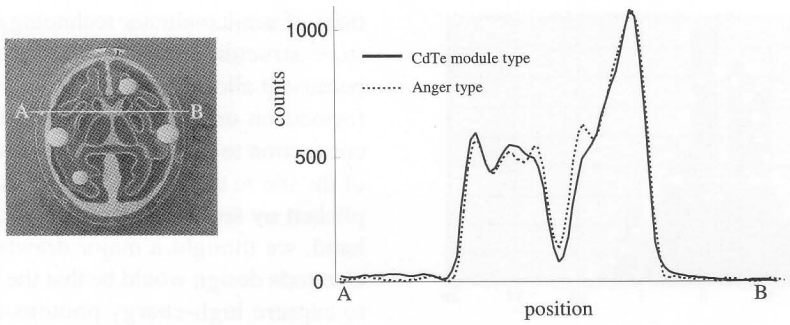

Fig. 7 The count profile curves of IMP brain phantom SPECT images. The signal levels of the images by CdTe detector and Anger-type, along the line, A–B. CdTe module type has slightly better contrast than Anger type.

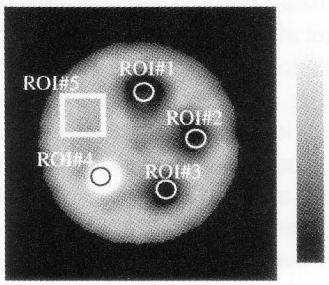

Fig. 8 SPECT image of the sphere phantom and the ROIs for measuring the SPECT image values. Hot sphere and warm background were filled with Tc-99m with the density ratio of 3.7 : 1. ROI#1 was set at 71 m*l* sphere. ROI#2 was set at 56 m*l* sphere. ROI#3 was set at 42 m*l* sphere. ROI#4 was set at the hot sphere. ROI#5 is set at background area.

the time from when the detector output crossed 40 keV to when another detector output crossed the same threshold level was measured. A total of 500 coincidence events were collected after discarding events that did not meet the criteria for coincidence that the measured energy should be higher than 450 keV.

Test environment

All measurements were performed at room temperature, controlled between 20 and 28 degrees Celsius. No special temperature control other than a room air conditioner was used. Humidity was not controlled but was below 80% relative humidity (RH).

RESULTS

Energy resolution

Excluding the defective elements, the average FWHM of 512 elements was 5.11% at 140 keV. The standard deviation was 0.80%, the maximum was 6.68% and the minimum 3.26%. As a representative of the 512 elements, the energy spectrum of one element with results close to the average is shown in Figure 2.

Table 1 Comparison of the sphere phantom values between SPECT images of the Anger-type camera and the CdTe detector module. The image and ROI positions are shown in Figure 8

	Ideal	Anger type	CdTe module
ROI#1	0	0.30	0.16
ROI#2	0	0.28	0.22
ROI#3	0	0.28	0.20
ROI#4	3.7	2.56	2.97

Intrinsic spatial resolution

The obtained image and count profile curve are shown in Figure 3. The intrinsic resolution of 1.6 mm was confirmed by using a bar phantom.

Line spread function

FWHM of the images from the line source is shown in Figure 4. For comparison, the theoretical FWHM of the Anger type is also shown.

Sensitivity

With the LEHR collimator, the measured sensitivity of the CdTe detector module with a 10% window was 78% of that of the NaI detector with a 20% window. The variation in sensitivity for every pixel was within 4.7%.

Planar image of IMP brain phantom

The planar images of the brain phantom are shown in Figure 5, for both the CdTe detector module and the Anger type. Though there is some microscopic unevenness for which the sensitivity calibration did not work perfectly, the image from the CdTe detector is visibly superior in contrast and sharpness.

SPECT image of IMP brain phantom

The SPECT images are shown in Figure 6 for the CdTe detector module with the LEHR collimator and for the Anger type. The quality of the image from the CdTe detector module is slightly different from that from the Anger camera. The signal level profiles from identical

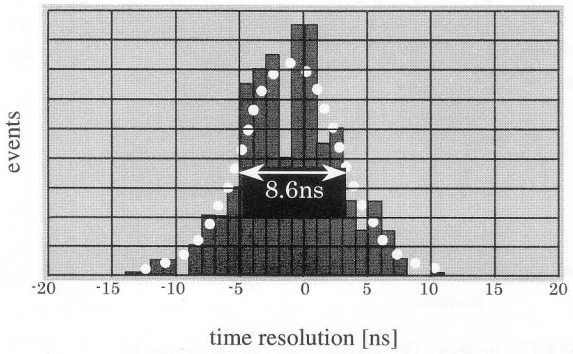

Fig. 9 Coincidence time resolution or the time difference of two detector pieces. Gaussian profile is fitted to the histogram and the FWHM of fitted profile is 8.6 ns. Leading edge triggering method was used.

locations in these images are shown in Figure 7, and the difference in the profiles reinforces the visible difference between the images.

SPECT image and quantitative data of sphere phantom
The regions of interest (ROIs) used to measure the SPECT image value of the spheres are shown in Figure 8, and their quantitative summary is shown in Table 1. The image from the CdTe detector module shows values substantially closer to the ideal as compared to those from the Anger type camera.

Coincidence time resolution
The histogram of the time difference between the two CdTe detector pieces is shown in Figure 9. A bin size of 1 ns was used to bin the measured time differences in generating this histogram. A Gaussian fit was then applied to the histogram, and the result gave an FWHM of 8.6 ns.

DISCUSSION

Design of detector element and detector module
In this study, the design objective was to pursue the maximum possible performance as a radiation detector over ease of fabrication. We reviewed previously reported designs of a semiconductor detector for the gamma camera and decided to take a considerably different approach. One major difference was the material. During the past several years, CZT has been the first choice as the semiconductor material for a radiation detector because of its high resistivity that allows application of a high bias voltage for efficient charge collection. Nevertheless, we chose CdTe because recent reports had shown that progress in blocking-contact technology for CdTe would allow much higher bias voltages while suppressing dark current to reasonable levels.[9–11]

Another major difference was the choice of the vertical electrode structure over the horizontal electrode structure that has been the first choice for gamma camera applications of semiconductor technology. The horizontal electrode structure simplified detector module fabrication because it allows a two-dimensional multi-element to be formed on one semiconductor tile, and the electrical connection to the signal electrodes formed at the bottom of the tile to the charge amplifiers can be easily accomplished by solder-bumping, for example. On the other hand, we thought a major drawback of the horizontal electrode design would be that the tile thickness required to capture high-energy photons efficiently would not allow collection of a sufficient amount of charges, especially holes, and that the energy resolution would be compromised as a result. Granted, the "small-pixel-effect"[3,12] would help minimize the effect of insufficient collection of holes. Indeed, energy resolutions better than those for our data have been obtained already by applying the small pixel effect to a CZT tile with a thickness of 5 mm^3. Nevertheless, this detector was only a 4×4 array with a guard ring, and its structure as is may not be suitable for a detector with a large enough area for experimental imaging, not to mention for an ordinary gamma camera. As far as we are aware, reported energy resolutions of the CZT tile with large enough array sizes have been only slightly better than those of the Anger-type camera. Furthermore, we were in pursuit of thickness that would allow for mid- to high-energy photons and coincidence detection would be very difficult with a horizontal tile structure since the charges must drift a length of 5 mm or more, and thereby response speed would be significantly worsened.

On the other hand, the vertical electrode structure gives us freedom of detector depth because the charge collection distance between the bias electrode and signal readout electrode is orthogonal to and independent of the detector depth. We chose a small element pitch of 1.6 mm and an electrode distance of only 1.35 mm to minimize the charge drift time and allow almost 100% charge collection efficiency for both electrons and holes.

One of the reasons why CdTe has been less preferred than CZT is the polarization phenomenon. The resistivity of CdTe is relatively low, and blocking contact is required to apply high-bias voltage while suppressing dark current. If blocking contact is used, it is almost always accompanied by the polarization problem.[13–15] With polarization, the performance of the detector degrades gradually with time in use. Nevertheless, a polarized detector can return to its normal state by having the bias voltage switched off for a short while,[9,14] and for use in nuclear medicine in general, switching off momentarily every 10 or 20 minutes would usually be acceptable. CdTe is therefore a very promising material for nuclear medicine even at the present level of material technology.

Energy resolution
The energy resolution obtained, an average FWHM of 5.1% at 140 keV, is satisfactory, considering that the NaI-

based Anger camera has an FWHM of about 10% at best, but theoretically, the energy resolution of the CdTe detector should be far better. In other areas in which only a few CdTe elements are necessary, CdTe crystals can be carefully chosen. In those areas, substantially better results have been reported. For gamma camera applications, with a large quantity of semiconductors necessary, the cost would be prohibitive if only choice detectors could be used. Without having to resort to such measures, however, we are certain that better energy resolution can be obtained by using knowledge gained about handling CdTe detectors during the fabrication process in the study. With careful handling and new module structure design, we may be able to obtain an average energy resolution close to 3.3% at 140 keV, which is the best obtained value with our present 512 elements detector.

Another important item to note in the energy spectrum is that there is no obvious tailing. Very often semiconductor detectors performing poorly show a significant response at the lower side of the energy peak. Called tailing, it results in the peak-energy events' being counted as lower energy and leads to lower sensitivity, unless the energy window for acquisition is set several times wider than the FWHM.

Spatial resolution

Considering that the sampling frequency determined by element pitch is 1/1.6 mm^{-1} and that the basic component of phantom spatial frequency is 1/4.5 mm^{-1} when placed at 45 degrees, it may be a matter of course to resolve the 1.6 mm bar phantom. But it is important to note that this intrinsic resolution indicates that there is no substantial dispersion of charge clouds straddling the detector elements. This may be another advantage of the vertical electrode structure over the multi-element tile design with a horizontal electrode structure.

It is expected that the benefit of high intrinsic resolution cannot be taken advantage of fully when a collimator is used and the object is at a certain distance from the detector. Nevertheless, improvement in spatial resolution of the CdTe detector compared to that of the Anger camera was not insignificant when the distance was shorter than about 100 mm.

Sensitivity

Though we could not find any published evidence, we seem to recall that some of the experimental semiconductor detectors intended for gamma-camera use had shown substantially lower sensitivity than NaI because of tailing. In this study, even though there was no obvious tailing in the energy spectrum (Fig. 2), the measured sensitivity 78% of NaI might not seem good enough at first glance, but since LEHR was asynchronous with the detector array, we then needed to take geometric efficiency into account. The ratio between the surface area of the semiconductor element and the dead space of the element gap was 0.77. This suggested that our detector module was virtually free from tailing and resultant sensitivity loss. With a synchronous collimator, the sensitivity of our detector module would be about equal to that of NaI at half the energy window width and higher than NaI at a comparable energy window width.

IMP brain phantom

In the planar images, since the object was only 50 mm away from the detector, high spatial resolution of the CdTe detector would contribute to the superior image quality. In the SPECT images, since the radius of the camera head orbit is 132 mm, the spatial resolution with a CdTe detector is almost the same as with the Anger type. The difference in image quality can be better explained by the difference in the profiles in Figure 7 that shows higher contrast in the image with the CdTe detector. It is natural to conclude that this difference in contrast is caused by the difference in the scatter component because the energy window of the CdTe detector module was only 10%, half that of the Anger camera. In other words, the high energy resolution of the CdTe detector is most likely to be the main reason for good image contrast.

SPECT image of sphere phantom and its quantitative data

Quantitative assessment with the sphere phantoms suggested a substantial advantage of the CdTe detector over the Anger camera. Owing to higher energy resolution or narrower window width, the image by the CdTe detector gave closer values to the ideal than the Anger type when both were not corrected for scatter.

In one area, there seems to be room for further investigation. The window width of the CdTe detector is half that of the Anger type, so that we had at first expected that the scatter contribution would be halved. Since the SPECT image reconstruction process should be mathematically linear, the resulting quantitative data for the CdTe detector would be around mid-range between the ideal and the values in the NaI data. But actually, data from the CdTe detector included values slightly worse than mid-range, as shown in Table 1. The partial volume or blurring effect is too small to explain the difference between the theoretical and actual data.

Despite this remaining question, we believe that the importance of high energy resolution of the semiconductor has been demonstrated again by this experiment.

Coincidence time resolution

We believe that the FWHM of 8.6 ns obtained for coincidence in this study may not be the best value possible with our present detector. If we had used a more elaborate triggering scheme such as the constant fraction method rather than the simple leading-edge method, perhaps we could have obtained a better value. With the present technology, however, it would have been a major challenge to implement such a complex scheme for 128

detectors in one ASIC and the value of 8.6 ns is not very reliable from a statistical viewpoint because the total number of events was only 500. In addition, these data were obtained by using a makeshift tool with discrete-charge amplifiers, and we emphasize that we intended this experiment to be only an initial investigation, and that to conduct a proper study, data should be gathered with an ASIC more suited for compatible with coincidence detection. Nevertheless, since the time windows used for coincidence detection in most PET and coincidence-augmented SPECT imagers are typically 10 ns or more, the FWHM of 8.6 ns obtained in this study seems to be acceptable.

This time resolution is owing to high bias voltage and the short distance between the bias and signal electrodes, i.e., the blocking contact and vertical electrode design. Both electron mobility and the hole mobility of CZT are slightly better than those for CdTe, and, therefore, the coincidence time resolution of CZT may be slightly better than that of CdTe in theory. Nevertheless, the blocking-contact technology for CZT does not seem be sufficiently developed, and it would be difficult to apply sufficiently high bias voltage while keeping dark current at the low level which is required for lower energy imaging. We believe that our data have shown that the CdTe detector designed for gamma-camera imaging has the potential to function reasonably well for PET imaging also.

With a CdTe depth of 8 mm, the stopping power for 511 keV photon is only comparable to that of NaI with a depth of 16 mm, and detection efficiency may still not be satisfactory, depending on the performance desired for PET imaging. This is because the atomic number of CdTe is still not high enough for 511 keV, and Compton scattering is predominant. But by combining the dispersed energies from nearby detector elements from the same time window and counting them as a valid event if the total energy is about 511 keV, it may be possible to improve sensitivity.[16]

CONCLUSION

We have demonstrated the advantages of the semiconductor detector over the Anger-type gamma camera by using a CdTe detector module with blocking contact and vertical electrode structures. The most important advantage is the energy resolution and resulting superior image quality and quantitative accuracy of SPECT images.

We have also demonstrated that the time resolution of coincidence detection by the CdTe detector designed for gamma-camera use would be within the acceptable range for ordinary PET imaging.

ACKNOWLEDGMENTS

The authors wish to express their appreciation to R. Ohno and other engineers at Acrorad (Japan) for their cooperation in the fabrication of the CdTe detector element and module.

REFERENCES

1. Schlesinger T, Jones R. Semiconductors & semimetals: semiconductors for room temperature nuclear detector applications. Academic Press, 1995.
2. Butler JF, Lingren CL, Friesenhahn SJ, Doty FD, Ashburn WL, Conwell RL, et al. CdZnTe Solid-State gamma camera. *IEEE Trans Nucl Sci* 1998; NS-45: 359–363.
3. Bennett PR, Shah KS, Cirignano LJ, Klugerman MB, Dmitryev YN, Squillante MR. Multi-element CdZnTe detectors for gamma ray detection and imaging. *IEEE Trans Nucl Sci Symp Conf Rec* 1997; 561–564.
4. Matherson KJ, Barber HB, Barrett HH, Eskin JD, Dereniak EL, Marks DG, et al. Progress in the development of large-area modular 64 × 64 CdZnTe imaging arrays for nuclear medicine. *IEEE Trans Nucl Sci* 1998; 45 (3): 354–358.
5. Ozaki T, Iwase Y, Takamura H, Ohmori M. Thermal treatment of CdTe surfaces for radiation detectors. *Nucl Instr and Meth* 1996; A380: 141–144.
6. Funaki M, Ozaki T, Satoh K, Ohno R. Growth and characterization of CdTe single crystals for radiation detectors. *Nucl Instr and Meth* 1999; A436: 120–126.
7. Takayama T, Nakamura N, Motomura N, Mori I, Ozaki T, Ohno R. Feasibility study of SPECT quantification using CdTe semiconductor detector. *KAKU IGAKU (Jpn J Nucl Med)* 2000; 37: 333–338.
8. Takayama T, Hiwatashi K, Nakamura N, Motomura N, Mori I, Ozaki T, et al. Feasibility study of CdTe semiconductor detector for gamma camera. *KAKU IGAKU (Jpn J Nucl Med)* 2000; 37: 181–187.
9. Takahashi T, Hirose K, Matsumoto C, Takizawa K, Ohno R, Ozaki T, et al. Performance of a new Shottkey CdTe detector for hard X-ray spectroscopy. *SPIE* 1998; 3446: 29–37.
10. Matsumoto C, Takahashi T, Takizawa K, Ohno R, Ozaki T, Mori K. Performance of a new Shottkey CdTe detector for hard-X-ray spectroscopy. *IEEE Int Nucl Sci Symp* 1997; 1: 569–573.
11. Niraula M, Mochizuki D, Aoki T, Tomita Y, Nihashi T, Hatanaka Y. Development of high-resolution CdTe radiation detectors in a new M-π-n design. *IEEE Trans Nucl Sci* 1999; 4: 1237–1241.
12. Barrett HH, Eskin JD, Barber HB. Charge transport in arrays of semiconductor gamma-ray detectors. *Phys Rev Letters* 1995; 75: 156–159.
13. Lachish U. CdTe and CdZnTe semiconductor gamma detectors equipped with ohmic contacts. *Nucl Instr and Meth* 1999; A436: 146–149.
14. Matz R, Weidner M. Charge collection efficiency and space charge formation in CdTe gamma and X-ray detectors. *Nucl Instr and Meth* 1998; A406: 287–298.
15. Bell RO, Entine G, Serreze HB. Time-dependent polarization of CdTe gamma-ray detectors. *Nucl Inst and Meth* 1974; 117: 267–271.
16. Ohtani M, Ogawa K, Takayama T, Mori I. Improvement of detection efficiency in coincidence data acquisition with CdTe detector. *IEEE Trans Nucl Sci* 2001; (in press).